Vision, Modeling, and Visualization (2014)
J. Bender, A. Kuijper, T. von Landesberger, H. Theisel and P. Urban (Eds.)

Combined Three-Dimensional Visualization of Structural Connectivity and Cortex Parcellation

A. Reichenbach[1], M. Goldau[1], and M. Hlawitschka[2]

[1]Image and Signal Processing Group, Computer Sience Institute, Leipzig University, Germany
[2]Scientific Visualization Group, Computer Sience Institute, Leipzig University, Germany

Abstract

The human cortex is organized in spatially distinct regions of different functional units. Cortex parcellations based on magnetic resonance imaging (MRI) of living human subjects are common practice, and recently, structural connectivity from diffusion weighted resonance imaging (dwMRI) have been successfully applied to generate such parcellations. The exploration of structural connectivity data together with cortex parcellations has proven to be challenging due to overlapping tracts and structures, limited depth perception, and the large number of tracts, which clutter the visualization. However, the involvement of structural connectivity forces such visualizations to act in anatomical space. While structural connectivity can be communicated using three-dimensional or slice-based visualizations, cortex parcellations are visualized on three-dimensional surfaces. In this work, we solve this problem by proposing an interactive illustrative 3D visualization for both structural connectivity data and cortex parcellations in anatomical space. We achieve this by providing an abstract visualization of the structural connectivity while still being able to provide the full detail on demand. Our visualization furthermore employs interactivity and illustrative depth-enhancing, which are supported by anatomical context and textual annotations and thus help the user to build a mental map of the connections in the brain. Functional and effective connectivity might benefit from such a combined visualization as they use cortex parcellations as well.

Categories and Subject Descriptors (according to ACM CCS): I.3.3 [Computer Graphics]: Display algorithms—

1. Introduction

The understanding of brain connectivity is a major goal of neuroscience. Therefore, among others, structural and functional connectivity is analyzed. Structural connectivity describes the physical connections between the different regions in the brain, whereas the functional correlation between distinct regions of the brain is indicated by functional connectivity. While it has been shown that different cortical areas are linked to different functions, cortex parcellations are of utmost importance to neuroscientists.

The advent of magnetic resonance imaging (MRI), diffusion weighted MRI (dMRI), and functional MRI enables us to analyze brain connectivity in the living subject without substantial harm. Structural brain connectivity may be estimated from dMRI data with tractography. Current tractography methods reconstruct three-dimensional white-matter tracts either as probability-like scalar field or as polyline data (cf. Behrens et al. [BSJ14]). Additionally, cortex parcellations might be estimated directly from structural MRI data (T1-weighted and T2-weighted MRI), but can also be inferred from the analysis of structural connectivity data (cf. FreeSurfer [DFDH10], Gorbach et al. [GSJ*12], and Moreno-Dominguez et al. [MDAK14].)

Even though many publications study those data, a fully integrated visualization is rare and many recent publications rely on juxtapositions to communicate the findings (Fig. 1 shows examples of recent visualizations). Our aim is to present those data in an intuitive and interactive visualization system. The key elements comprise

- the spatial visualization of neural fibers,
- the representation of cortical structures,
- efficient visual encoding of relations between structures,
- interactive queries and automatic labeling, and
- anatomical context by T1-slices and cortex information.

DOI: 10.2312/vmv.20141278

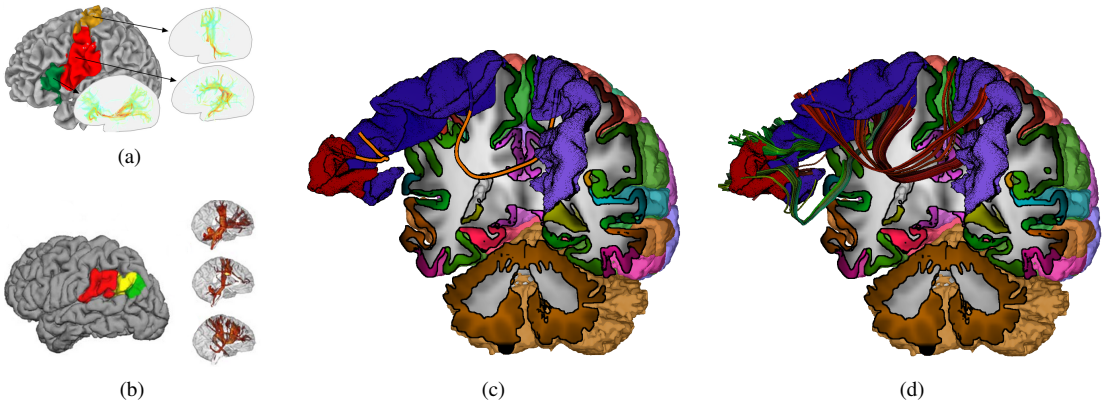

Figure 1: *Images (a) and (b) show typical visualizations of cortex parcellations and corresponding structural information. (a) is taken from Gorbach et al. [GSJ*12] and (b) is taken from Moreno-Dominguez et al. [MDAK14]. With our visualization, we are able to depict cortex parcellation and structural connectivity within one visualization ((c) and (d)).*

2. Related work

2.1. Visualization of connectivity

Deterministic diffusion tractography, as for example proposed by Mori et al. [MCCVZ99], traces paths of least hindrance of diffusion through the diffusion dataset. The resulting paths are often rendered as a dense set of a high number of lines, where the number may be anything from a few hundred to millions. This leads to a high amount of visual clutter and occlusions. Many different line rendering methods have been proposed and applied to the rendering of the tract data. Zhang et al. [ZDL03] draw the line data as tubes while culling the lines to make the representation more sparse. More advanced approaches try to help the user to identify structures and spatial relations in the dense line data, for example by adding *depth-dependent halos* [EBRI09], or by applying ambient occlusion [EHS13a].

Visualizations in anatomical space are suitable for conveying spatial relations of cortex regions and connecting fiber bundles. Such visualizations were also published for functional connectivity, which describes correlations in the activity of these gray matter regions. Worsley et al. [WCLE05] render functional magnetic resonance (fMRI) activation regions as colored meshes and represent correlations in activity by cylinder-shaped connections. Context is provided by a transparent mid-cortical surface. These representations result in very cluttered images, especially in locations with many similar connections. Böttger et al. [BSL*13] reduce regions of interest (ROIs) to a point in anatomical space and render correlations in the form of lines. Using mean-shift edge bundling, edges that connect similar regions are bundled in a way that reduces the space required to draw them and visually separates bundles connecting different regions. Coloring bundles further improves readability. However, due to the lack of anatomical information, these approaches cannot be directly applied to structural connectivity.

2.2. Illustrative techniques

Techniques using the traditional illustration of medical and anatomical textbooks (e.g. [MVA07]), such as stippling and hatching, have been emulated on the computer for visualization purposes. An overview on the different methods can be found in [PB07]. Born et al. [BJH*09] divide context geometry into a solid and a transparent part along a slice and relate fiber data along with fMRI measurements. Everts et al. [EBRI09] add depth cues by rendering halos, whose size depends on the difference in depth to neighboring fibers along the fiber's paths. This helps the viewer to visually cluster the fibers into bundles and to identify the spatial relations; however, this approach does not solve the occlusion problem and also lacks context information. Svetachov et al. [SEI10] solve these problems by adding context geometry to the image. They use hatching to convey the shape of the outer surface of the brain and stippling to render the gray matter inside the cut out part. While this makes gray matter regions of interest easy to identify, it only works for a small number of bundles which are additionally occluded by the context geometry. Otten et al. [OVVDW10] draw a representation of the surfaces that enclose clustered fiber bundles using a screen space method. Shape perception is enhanced by drawing outlines and feature lines, and hint lines inside the surface convey the directions of the fibers. An exploded view helps avoiding the occlusion problem but distorts the space. Goldau et al. [GWG*11] render stipples in anatomical slices to combine directional information from diffusion tensors with probability values from probabilistic tractography. Context is shown only in the form of gray and white matter outlines. Multiple probabilistic tractograms can be viewed

at the same time and are differentiated by color. As with all slice based visualizations, this avoids the clutter issue, but lacks expressive context and thus depends on the viewers anatomical "mental map". Röttger et al. [RMM12] abstract fiber bundles into hulls that contain the bundled tracts. Bundles can be rendered as a set of fibers or only their hull geometry. Cutaway views are used to make fibers visible that are contained inside a hull. They apply a color coding to convey the depth of the fiber inside the hull. Due to the large amount of screen space occupied by single hull representations in [OVVDW10], the images can contain a lot of clutter when showing many bundles at the same time.

Further methods that may be interesting for structural connectivity stem from the illustrative visualization of vascular systems. These can be seen as structures of branching lines that have a diameter varying along the lines. Ritter et al. [RHD*06] introduce techniques for conveying distance and spatial orientation of such structures. *Distance-encoded shadows* show the distance of occluders to hidden objects by changing the shadow's length and shade depending on the distance. *Distance-encoded surfaces* convey the distance of the structure to the viewer by changing the strength of a regular pattern drawn on the vessels. The distance to important regions (e.g. tumors) is depicted by modulating the strength of a procedural texture on the surface of the vessel with the distance to the object. Hansen et al. [HWR*10] also introduce *distance-encoding silhouettes*, changing the thickness of the vessel's silhouettes with their position along the view direction. Also, they change rendering styles of the silhouettes depending on whether the vessel penetrates a target structure such as a tumor. These techniques help identifying the spatial relations both within the vessel structure and between vessels and objects.

2.3. Annotations

Annotations provide important information on objects in a scene or on a map, such as the names of the objects. They are frequently used in anatomy books in order to link ROIs in the illustrations to their descriptions in the text. The labeling problem can be described as placing labels near an object or an anchor point, such that both label content and leader lines do not intersect. Unfortunately, even the simplest formulations of the labeling problem are NP–hard [MS91]. There have been different approaches to solving the problem: force–based methods [VTW12], genetic algorithms [YL05], fuzzy optimization [ČB10], greedy heuristics [Mot07] and others. Jainek et al. [JBB*08] use a labeling algorithm which places labels close to the cortex areas based on their alpha shapes. Stein et al. [SD08] propose an image-space real-time labeling algorithm implemented mainly on the GPU. They choose label positions using a cost function and the order in which to process the labels using a greedy strategy. The positions to avoid placing labels at can be supplied as a texture. Its general formulation and the use of the cost function makes the algorithm easy to apply to different data.

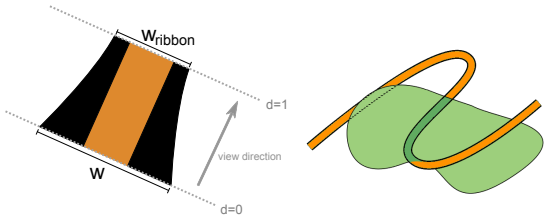

Figure 2: *We use two encodings for visualizing spatial information. Left: The ribbon width changes to emphasize the depth encoding. The parameter w_{ribbon} denotes the minimal width. The width w at every position along the path is then calculated from w_{ribbon} and the depth d along the view direction. Right: Bundle boundaries are stippled when they are behind surfaces. The bundle color changes according to the area it traverses, and has a solid color when in front of all other geometry.*

3. Methods

We first describe the input data required for our system, then we focus on our novel visualization.

3.1. Data and Preprocessing

The input data required for the visualization are a cortex parcellation providing a region identifier for each voxel and a set of fibers traced by a tractography algorithm. The data must be registered to the same space and colors and a name and type (white or gray matter) must be provided for every region. Optionally, a structural MRI dataset may be provided to add further detail. In case this is not provided as separate input data, we compute a connectivity graph based on the individual fibers by identifying all fibers that connect areas of the cortex parcellation.

For each region of the parcellation, we generate a mesh using marching cubes. To improve the quality of the surfaces, we apply the mesh smoothing algorithm of Jones et al. [JDD03] (parameters: $\sigma_{\text{dist}} = 0.1, \sigma_{\text{infl}} = 0.2$).

3.2. Visualization

The main steps of the rendering pipeline and their resulting images are presented in Fig. 3 and will be described in detail throughout the section. Our implementation is based on OpenGL multi-pass rendering to achieve interactive frame rates. All shaders have been implemented in OpenGL's shading language *GLSL*. Our implementation of the visualization will be freely available as an open source plugin to our visualization toolkit *OpenWalnut* [EHS13b].

We first describe the rendering techniques chosen for the

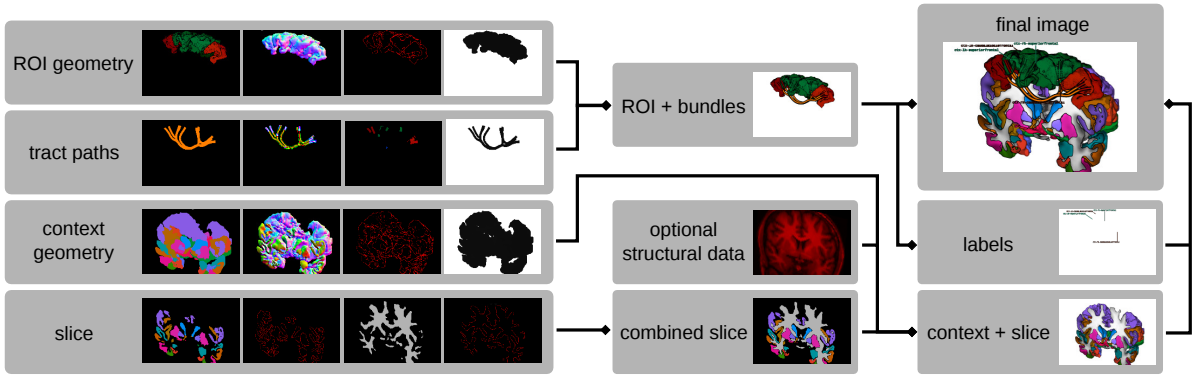

Figure 3: *Our multi-pass rendering pipeline: ROI and context are rendered individually and color, normals, silhouette, and depth are stored in textures. For the tracts, color, rendering detail, and ROI colors, and depth are stored. For the slice, only color and silhouette information is required. ROI combined with bundles are input for the label placement and the two are combined with the slice input in a final rendering pass.*

key aspects of our system before describing the interaction framework.

Regions of Interest. To study the connectivity, the user can select one or multiple cortex areas to either see fibers connecting those areas or to display fibers projecting into one of those areas. In this paper, we refer to those selected areas as Region of Interest (ROI), whereas other areas are seen as context geometry. The ROIs are rendered as solid objects using the color provided in the segmentation data. Even though this reduces the degrees of freedom we have in our visualization and may restrict the optimal presentation, it is helpful when comparing results generated by our visualization to those of other tools.

However, in order to help the user understand the spatial relations between all ROIs, we also want to employ color to depict the ROI's depth along the viewing direction. This is achieved by changing the color's luminance depending on the distance to the viewer relative to the position of the data's bounding box, so that objects closer to the viewer will appear brighter. The relative depth of each fragment is calculated as

$$d = \frac{1}{2} - (\vec{t} - (\frac{1}{2}, \frac{1}{2}, \frac{1}{2})^T) \cdot M_{MV}^{-1} e_z,$$

where $\vec{t} \in [0,1]^3$ is the coordinate of the fragment inside the brain's bounding box, e_z is the respective unit base vector for the z-coordinate and M_{MV}^{-1} is the inverse of the modelview matrix. By using this depth value to scale the luminance between 50% and 20%, we utilize the known relationship of luminance to depth perception [LB99].

Secondly, we further emphasize the object's shape by drawing black outlines along the silhouette ROI geometry and applying an illustrative shading. Due to the complex shape of the meshes, hatching along the main curvature directions did not provide satisfactory results. For this reason, we chose to add further shape hints with a stippling technique instead. The stippling uses a standard 2D texture mapping approach as is used for *tonal art maps*. We use an approach that projects the respective point's normal onto the nearest side of a cube mapped with a texture on every side and then use that projected point's texel color. We create the required texture by means of Turing integration as used by Eichelbaum et al. [EHHS12]. This provides a texture containing both evenly spaced and well-distributed points. While there are more complex approaches described in the literature (e.g. [BTBP07]), it proved to be sufficient for our purposes.

Tract Bundle Paths. As default in our system, we decided against rendering the full tract geometry in order to reduce clutter and occlusion. The approaches of [OVVDW10] and [RMM12] take up large amounts of screen space. Instead, we compute a centerline for every cluster by averaging all fibers that belong to the cluster. This abstraction allows us to convey the approximate path of a bundle while using a minimal amount of screen space. Motivated by the results of Hansen et al. [HWR*10], the mean path is rendered as view–aligned ribbon having outlines of depth-dependent thickness. To improve depth perception, we calculated the ribbon's width as

$$w = w_{\text{ribbon}} \cdot (1 + 3 \cdot (1 - d)^2)$$

with the depth value d, and $w_{\text{ribbon}} > 0$ is the ribbon width parameter (cf. Fig 3 left). Whereas a natural scaling would require a linear scaling with depth, we use a quadratic term to over-emphasize the depth information and to improve comparability. However, we keep the width of the inner part of the ribbon constant at 80% of the ribbon width, which leads to the boundaries of the lines carrying the emphasized depth information.

Unlike the situation in Hansen et al.'s work and depending on the configuration of the scene, we may have multiple visible cortex areas that occlude each other and the ribbons. In order to convey whether a tract is inside, in front, or behind a single ROI, we encode this information using the color of the inner part of the ribbon and the boundary (cf. Fig. 3 right): For an unoccluded ribbon, we draw normal outlines and fill the inner part with a color chosen by the user. If a tract is not inside a ROI geometry, but occluded nonetheless, we only draw stippled outlines. Should a ribbon penetrate a ROI, we fill its inner part with the color of the ROI it is crossing. This color lookup for the ribbons is based on a three-dimensional texture containing the parcellation identifiers and is performed during the rendering of the ribbons.

3D Context. Three different styles are available for the display of the context, trading shape perception for screen space usage:

1. A fully opaque style employing a standard toon shading. This is useful for active ROIs.
2. A glass brain style that calculates the transparency from the light factor as in the standard Phong lighting model. Surfaces parallel to the view plane are fully transparent while the edges of the geometry are opaque.
3. A minimalistic style rendering only the silhouette of the context.

Going from style 1 to 3, the abstraction level increases, shape perception and context information become weaker as the ROIs become less occluded, and the final image becomes less cluttered. The colors of the context meshes are converted into the HSL color model and their luminance and saturation are set to 50% and 80%, respectively. To minimize clutter, we only render the front facing part of the cortex regions.

Slicing. As neuroscientists are trained to use slice-based views, which may provide more detailed anatomical context and allow to also view subcortical gray matter regions, we implemented cutting slices to remove distracting context geometry. Within the slice, the ROIs are made clearly distinguishable using their respective colors and outlines. Furthermore, the slice can be colored according to other scalar data such as structural MRI. Creating the slice requires rendering the back-facing geometry of the context regions that are not occluded by front-facing geometry.

Annotations. Just like in medical illustrations and for orientation purposes, the user can choose to display annotations for important regions of the final rendering. We require the labeling algorithm to be suitable and fast for a set of less than around 20 visible labels, as too many active ROIs and labels would only clutter the screen. As the visualization can be rotated and zoomed, label positions would ideally be frame-coherent. Annotations should to be placed as close as possible to their respective ROIs while avoiding occlusions with the ROI geometry. The labeling algorithm of Stein et al. [SD08] best suits these requirements. Our OpenCL implementation has punishing terms for label overlap and occlusion of highlighted areas in the brain and iteratively updates the positions when changing the point of view. The label's text and its leader line are rendered in the color of the respective ROI and a black shadow is added in order to provide contrast to both ROIs and the background of the image. Currently, we only display the labels provided by the cortex segmentation, but additional textural or graphical information could be shown as well.

Interaction. One key feature of our system is interactivity. To provide a high amount of flexibility, the visibility of all objects in the scene is determined by a set of configurable filters. The current selection of filters includes

- filters for selecting ROIs from the list of regions,
- filters for selecting all tracts incident to a selected region, and
- filters for removing tracts that have less than a threshold amount of fibers.

The system maintains a stack of filters which are applied to the data. All filters have access to the output of previous filters, interaction events such as picking on areas, and each filter can determine whether a region is selected as ROI or a tract should be shown. The activation of ROIs, for example, is implemented in one such filter that displays a list of all available cortex areas and handles multiple selections in that list as well as picking in the 3D scene. The selection of displayed fibers or ribbons can then be performed in a second filter that is based on the active ROIs chosen in the first filter, and so on. By manipulating the filter pipeline, users can easily adapt the system, including parts of the interaction metaphors, to their specific needs.

4. Results

In this section, we provide results of applying our technique to a real human brain dataset. Both HARDI and T1 structural data have been acquired on a 3T Tim Trio MRI scanner (Siemens, Erlangen). For the HARDI data, 60 gradient images were taken. Motion correction was applied by linearly registering to the intermediate $b = 0$ images and the fractional anisotropy was calculated for every voxel. The structural scan was then linearly registered to the FA image and a gray matter parcellation was generated using the *FreeSurfer* toolkit. Afterwards, fiber clusters were identified by finding the set of tracts connecting each pair of gray matter regions. The respective fibers were identified by testing whether the start and end points of the fibers were located in a gray matter region. If that was not the case, we extended the fiber by up to ten millimeters to check whether it would hit a gray

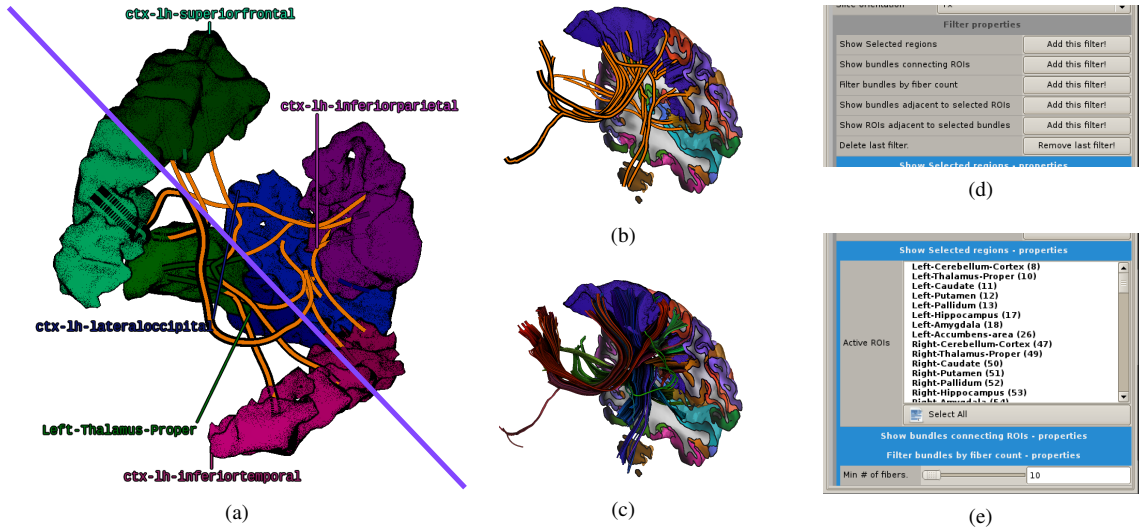

Figure 4: *Examples. (a) Rendering without (top right) and with (bottom left) depth–enhancing techniques. (b) and (c) Showing fiber bundles incident to the left precentral cortex with abstracted representation and in detail, respectively. (d) Filters can be added to or deleted from the filter stack with the press of a button. (e) Filters can react to picks in the scene and have their own options in the dialog. Newly added filters are put at the bottom of the list.*

matter voxel. This was needed to avoid false negatives due to registration errors. All fiber clusters were assigned random RGB colors for the purpose of telling them apart when rendering the bundle tracts in detail later on.

Figure 4 (a) demonstrates the effect of the depth–enhancing techniques. Relative depth of the bundles can easily be seen from the size of their outlines, as can be seen when comparing parts of the bundles on the left side (nearer) to those on the right side (deeper) of the bottom left part. Encoding the depth into the luminance allows to compare depth of regions even if there are no occlusions that would reveal their order along the view direction. The closest object to the viewer can be identified as the front part of the *superior frontal cortex*, as it has the highest luminance. Also note how we can easily identify whether a bundle is located behind (dotted) or within a selected region (full line). Subfigures (b) and (c) shows another scene with a different configuration of filters that displays all bundles that are connected to a cortex region. It demonstrates how the context geometry and slice are employed to improve orientation in the domain. It is also shown how the fibers composing the currently selected bundles can be rendered in detail using a range of common techniques, such as streamtubes and direction–encoding coloring. The filters that can be used to select the objects of interest can be applied, removed and modified in real–time. The GUI we use to do this is shown in subfigures (d) and (e).

During all interactions, we obtained interactive frame rates (58fps average without labels and 25fps with labels enabled during label placement on an NVIDIA GeForce 780M graphics card).

5. Discussion and Conclusion

While many of the techniques employed have been proposed by other groups, we achieved combining them into a new visualization with the purpose of conveying the connectivity of gray matter regions in the brain.

We provided a way to convey the location and path of tracts connecting different ROIs in the brain even in the presence of occlusions. Whether a tract runs through or behind any ROI can be seen at a glance, even if it is occluded by multiple ROIs at the same time. The different illustrative features make it much easier to perceive depth than in common volume visualization techniques. Through abstraction of fiber bundles into ribbons we reduce the huge amounts of visual clutter that plague most related visualizations. This allows to show more bundles of interest at the same time. Note, however, that this type of sparse representation leads to a loss of information. The shapes of the bundles are not represented at all and the end points of the centerlines do not accurately represent ”ending” locations of the tracked fiber bundles. Nonetheless, it allows to convey the connectivity patterns even in the presence of a large number of bundles. If more detail is required, the fibers of the selected bundles can be shown in full detail. For future work, we consider employing either a sheet–like representation capable of fanning or a skeleton representation that accurately captures the

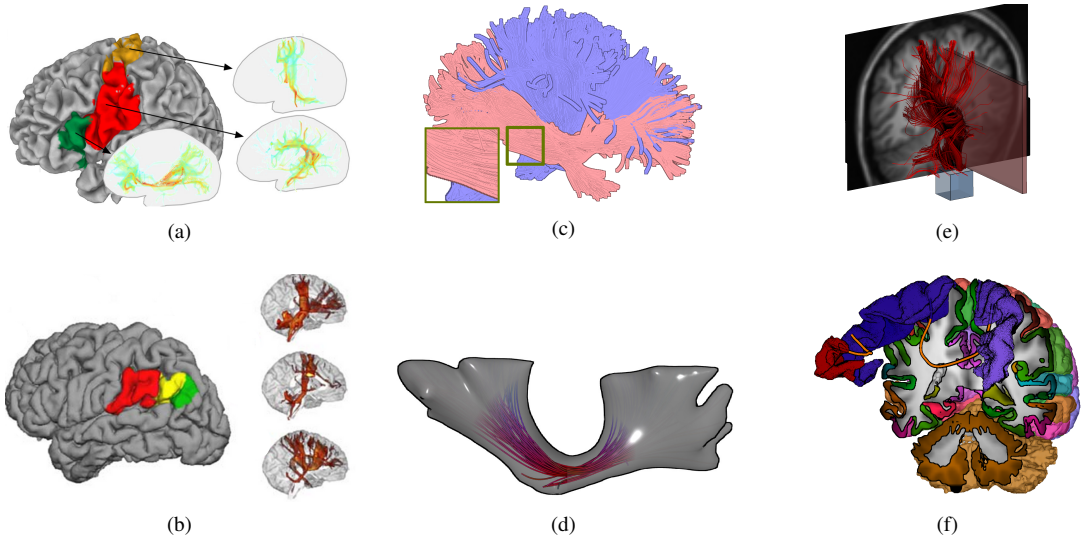

Figure 5: *Comparing to previous approaches. (a) and (b) are excerpts of manually arranged figures from [GSJ*12] and [MDAK14], respectively. (c) was created using the visualization of Otten et al. [OVVDW10]. (d) shows the visualization of Röttger et al. [RMM12]. (e) shows an example of a ROI based approach, where fibers are filtered by ROIs that can be placed in the domain. (f) is an example of a scene produced by our visualization.*

topology of the bundles. However, this may lead to more occlusions and clutter near the gray matter regions.

Another important aspect is providing context, which helps navigating in the visualization and gives cues to what regions may be interesting. A slice that can be moved through the data provides even more detail and context. The selection of objects has proven to be intuitive. All this can be achieved at interactive frame rates using consumer type graphics cards.

Figure 5 compares our work to the most related work from the literature and state-of-the-art approaches. The figures of Gorbach et al. [GSJ*12] and Moreno et al. [MDAK14] ((a) and (b)) are manually assembled juxtapositions, and thus not interactive. The visualizations of Otten et al. [OVVDW10] and Röttger et al. [RMM12] ((c) and (d)) both use much more screen space per fiber bundle, which leads to occlusions much faster than is the case for our technique. They also lack strong anatomical context. A typical workflow based on manually placable ROIs is demonstrated in (e). Usually, interesting regions are identified using some (e.g. slice-based) representation of the data. ROIs of various shapes are then placed and the fibers to show are selected by whether they touch a ROI or not. With our system, regions of interest can simply be picked from the available list, and the bundles to show are then evaluated by the filter system, which can be adapted with just a few clicks; this makes our system much easier to use. In contrast to the vascular illustrations of Ritter et al. [RHD*06] and Hansen et al. [HWR*10](not shown here), we can support more complex connectome networks. Even if multiple ROIs are drawn on top of each other, with our visualization, we can still perceive which ROIs are penetrated by the tract bundles due to the employed coloring of the bundles in these regions. Especially for non-expert users, annotations provided by our visualization greatly increase the readability of the images.

There are, however, a few open issues. The currently implemented labeling algorithm of [SD08] uses pre-specified anchor positions, which cannot always be chosen optimally. Adding a step that finds suitable anchor positions similar to [JBB*08] might improve labeling quality, but may also increase computation time. Furthermore, it is often the case that the centerlines used to represent the bundles run along very similar paths. Even though this is anatomically reasonable, it may lead to visually unappealing results and make neighboring bundles hard to distinguish.

Acknowledgements

This work was funded by Leipzig University. We thank Thomas Knösche and Alfred Anwander for their valuable feedback, Anna Vilanova for providing the tool to create images of their visualization and Dorit Merhof and Diana Röttger as well as Marc Tittgemeyer for providing images of their work. We also thank the anonymous reviewers for the thorough and helpful reviews.

References

[BJH*09] BORN S., JAINEK W., HLAWITSCHKA M., SCHEUERMANN G., TRANTAKIS C., MEIXENSBERGER J., BARTZ D.: Multimodal visualization of DTI and fMRI data using illustrative methods. In *Bildverarbeitung für die Medizin 2009*. Springer, 2009, pp. 6–10. 2

[BSJ14] BEHRENS T. E., SOTIROPOULOS S. N., JBABDI S.:. Second edition ed. Academic Press, 2014, ch. MR Diffusion Tractography, pp. 429–451. 1

[BSL*13] BOTTGER J., SCHAFER A., LOHMANN G., VILLRINGER A., MARGULIES D.: Three-dimensional mean-shift edge bundling for the visualization of functional connectivity in the brain. 2

[BTBP07] BAER A., TIETJEN C., BADE R., PREIM B.: Hardware-accelerated stippling of surfaces derived from medical volume data. In *Proceedings of the 9th Joint Eurographics/IEEE VGTC conference on Visualization* (2007), Eurographics Association, pp. 235–242. 4

[ČB10] ČMOLÍK L., BITTNER J.: Layout-aware optimization for interactive labeling of 3d models. *Computers & Graphics 34*, 4 (2010), 378–387. 3

[DFDH10] DESTRIEUX C., FISCHL B., DALE A., HALGREN E.: Automatic parcellation of human cortical gyri and sulci using standard anatomical nomenclature. *Neuroimage 53*, 1 (2010), 1–15. 1

[EBRI09] EVERTS M. H., BEKKER H., ROERDINK J. B., ISENBERG T.: Depth-dependent halos: Illustrative rendering of dense line data. *Visualization and Computer Graphics, IEEE Transactions on 15*, 6 (2009), 1299–1306. 2

[EHHS12] EICHELBAUM S., HLAWITSCHKA M., HAMANN B., SCHEUERMANN G.: *Fabric-like Visualization of Tensor Field Data on Arbitrary Surfaces in Image Space.* Springer-Verlag, Heidelberg, Germany/Dagstuhl Seminar 09302, 2009, 2012, pp. 71–92. 4

[EHS13a] EICHELBAUM S., HLAWITSCHKA M., SCHEUERMANN G.: LineAO — Improved three-dimensional line rendering. *IEEE Transaction on Visualization and Computer Graphics 19*, 3 (2013). 2

[EHS13b] EICHELBAUM S., HLAWITSCHKA M., SCHEUERMANN G.: Openwalnut: An open-source tool for visualization of medical and bio-signal data. *Biomedical Engineering/Biomedizinische Technik* (2013). URL: www.openwalnut.org. 3

[GSJ*12] GORBACH N. S., SIEP S., JITSEV J., MELZER C., TITTGEMEYER M.: Information-theoretic connectivity-based cortex parcellation. In *Machine Learning and Interpretation in Neuroimaging*. Springer, 2012, pp. 186–193. 1, 2, 7

[GWG*11] GOLDAU M., WIEBEL A., GORBACH N. S., MELZER C., HLAWITSCHKA M., SCHEUERMANN G., TITTGEMEYER M.: Fiber stippling: An illustrative rendering for probabilistic diffusion tractography. In *Biological Data Visualization (BioVis), 2011 IEEE Symposium on* (2011), IEEE, pp. 23–30. 2

[HWR*10] HANSEN C., WIEFERICH J., RITTER F., RIEDER C., PEITGEN H.-O.: Illustrative visualization of 3d planning models for augmented reality in liver surgery. *International journal of computer assisted radiology and surgery 5*, 2 (2010), 133–141. 3, 4, 7

[JBB*08] JAINEK W. M., BORN S., BARTZ D., STRASSER W., FISCHER J.: Illustrative hybrid visualization and exploration of anatomical and functional brain data. In *Computer Graphics Forum* (2008), vol. 27, Wiley Online Library, pp. 855–862. 3, 7

[JDD03] JONES T. R., DURAND F., DESBRUN M.: Non-iterative, feature-preserving mesh smoothing. In *ACM Transactions on Graphics (TOG)* (2003), vol. 22, ACM, pp. 943–949. 3

[LB99] LANGER M. S., BÜLTHOFF H. H.: Depth discrimination from shading under diffuse lighting. *Perception 29*, 6 (1999), 649–660. 4

[MCCVZ99] MORI S., CRAIN B. J., CHACKO V., VAN ZIJL P.: Three-dimensional tracking of axonal projections in the brain by magnetic resonance imaging. *Annals of neurology 45*, 2 (1999), 265–269. 2

[MDAK14] MORENO-DOMINGUEZ D., ANWANDER A., KNÖSCHE T. R.: A hierarchical method for whole-brain connectivity-based parcellation. *Human Brain Mapping* (2014). 1, 2, 7

[Mot07] MOTE K.: Fast point-feature label placement for dynamic visualizations. *Information Visualization 6*, 4 (2007), 249–260. 3

[MS91] MARKS J., SHIEBER S. M.: *The computational complexity of cartographic label placement*. Citeseer, 1991. 3

[MVA07] MAI J. K., VOSS T., ASSHEUER J.: *Atlas of the human brain*. Academic Press, 2007. 2

[OVVDW10] OTTEN R., VILANOVA A., VAN DE WETERING H.: Illustrative white matter fiber bundles. In *Computer Graphics Forum* (2010), vol. 29, Wiley Online Library, pp. 1013–1022. 2, 3, 4, 7

[PB07] PREIM B., BARTZ D.: *Visualization in medicine: theory, algorithms, and applications*. Morgan Kaufmann, 2007. 2

[RHD*06] RITTER F., HANSEN C., DICKEN V., KONRAD O., PREIM B., PEITGEN H.-O.: Real-time illustration of vascular structures. *Visualization and Computer Graphics, IEEE Transactions on 12*, 5 (2006), 877–884. 3, 7

[RMM12] RÖTTGER D., MERHOF D., MÜLLER S.: The bundle-explorer: A focus and context rendering framework for complex fiber distributions. In *Eurographics Workshop on Visual Computing for Biology and Medicine* (2012), The Eurographics Association, pp. 1–8. 3, 4, 7

[SD08] STEIN T., DÉCORET X.: Dynamic label placement for improved interactive exploration. In *Proceedings of the 6th international symposium on Non-photorealistic animation and rendering* (2008), ACM, pp. 15–21. 3, 5, 7

[SEI10] SVETACHOV P., EVERTS M. H., ISENBERG T.: DTI in context: illustrating brain fiber tracts in situ. In *Computer Graphics Forum* (2010), vol. 29, Wiley Online Library, pp. 1023–1032. 2

[VTW12] VAARANIEMI M., TREIB M., WESTERMANN R.: Temporally coherent real-time labeling of dynamic scenes. In *Proceedings of the 3rd International Conference on Computing for Geospatial Research and Applications* (2012), ACM, p. 17. 3

[WCLE05] WORSLEY K. J., CHEN J.-I., LERCH J., EVANS A. C.: Comparing functional connectivity via thresholding correlations and singular value decomposition. *Philosophical Transactions of the Royal Society B: Biological Sciences 360*, 1457 (2005), 913–920. 2

[YL05] YAMAMOTO M., LORENA L. A.: A constructive genetic approach to point-feature cartographic label placement. In *Metaheuristics: Progress as real problem solvers*. Springer, 2005, pp. 287–302. 3

[ZDL03] ZHANG S., DEMIRALP C., LAIDLAW D. H.: Visualizing diffusion tensor MR images using streamtubes and streamsurfaces. *Visualization and Computer Graphics, IEEE Transactions on 9*, 4 (2003), 454–462. 2